AGU PUBLICATIONS

Global Biogeochemical Cycles

RESEARCH ARTICLE

10.1002/2014GB004875

Key Points:
- Reservoirs are less efficient in retaining reactive Si than lakes
- On average, dams retain 20% of the input of reactive Si to reservoirs
- Reservoirs accumulate 5.3% of the global reactive Si loading to watersheds

Supporting Information:
- Readme
- Appendix S1, Tables S1–S3, and Figures S1–S3

Correspondence to:
T. Maavara,
tmaavara@uwaterloo.ca

Citation:
Maavara, T., H. H. Dürr, and P. Van Cappellen (2014), Worldwide retention of nutrient silicon by river damming: From sparse data set to global estimate, *Global Biogeochem. Cycles*, *28*, 842–855, doi:10.1002/2014GB004875.

Received 8 APR 2014
Accepted 22 JUL 2014
Accepted article online 25 JUL 2014
Published online 13 AUG 2014

Worldwide retention of nutrient silicon by river damming: From sparse data set to global estimate

Taylor Maavara[1], Hans H. Dürr[1], and Philippe Van Cappellen[1]

[1]Ecohydrology Research Group, Water Institute and Department of Earth and Environmental Sciences, University of Waterloo, Waterloo, Ontario, Canada

Abstract Damming of rivers represents a major anthropogenic perturbation of the hydrological cycle, with the potential to profoundly modify the availability of nutrient silicon (Si) in streams, lakes, and coastal areas. A global assessment of the impact of dams on river Si fluxes, however, is limited by the sparse data set on Si budgets for reservoirs. To alleviate this limitation, we use existing data on dissolved Si (DSi) retention by dams to calibrate a mechanistic model for the biogeochemical cycling of DSi and reactive particulate Si (PSi) in reservoir systems. The model calibration yields a relationship between the annual in-reservoir siliceous primary productivity and the external DSi supply. With this relationship and an estimate of catchment Si loading, the model calculates the total reactive Si (RSi = DSi + PSi) retention for any given reservoir. A Monte Carlo analysis accounts for the effects of variations in reservoir characteristics and generates a global relationship that predicts the average reactive Si retention in reservoirs as a function of the water residence time. This relationship is applied to the Global Reservoirs and Dams database to estimate Si retention by damming worldwide. According to the results, dams retain 163 Gmol yr^{-1} (9.8 Tg SiO_2 yr^{-1}) of DSi and 372 Gmol yr^{-1} (22.3 Tg SiO_2 yr^{-1}) of RSi, or 5.3% of the global RSi loading to rivers.

1. Introduction

Silicon (Si) is an essential nutrient element for numerous aquatic organisms, foremost diatoms [*Conway et al.*, 1977; *Tréguer et al.*, 1995; *Van Cappellen*, 2003]. The availability of Si is therefore a key variable controlling the ecology and health of many aquatic environments, including rivers, lakes, and the coastal zone [*Billen et al.*, 1991; *Conley et al.*, 1993; *Koszelnik and Tomaszek*, 2008; *Schelske and Stoermer*, 1971; *Tavernini et al.*, 2011]. A growing number of studies have highlighted the effects of human modifications of stream and river systems, in particular the building of dams, on Si retention and the resulting consequences for regional to global-scale nutrient cycling and ecological processes [*Beusen et al.*, 2009; *Conley et al.*, 1993; *Garnier et al.*, 2010; *Harrison et al.*, 2012; *Hartmann et al.*, 2011; *Humborg et al.*, 2000; *Laruelle et al.*, 2009; *Teodoru and Wehrli*, 2005; *Thieu et al.*, 2009]. As ongoing construction of dams continues to increase the global volume of reservoirs, it is important to develop a predictive understanding of the accompanying impacts on Si fluxes along the river continuum.

Silicon is supplied to reservoirs under both dissolved and particulate forms. While diatoms and other siliceous organisms can directly take up dissolved Si, many Si-containing solid phases, including quartz and silicate minerals, are unavailable for biological utilization [*Cornelis et al.*, 2011; *Dürr et al.*, 2011; *Iler*, 1979]. A fraction of particulate Si, however, is supplied as reactive solid and solid-bound forms that can potentially act as a source of soluble Si in reservoirs. Diatoms and riparian plants further contribute to the particulate reactive Si pool of a reservoir through the production of biogenic silica [*Sauer et al.*, 2006; *Triplett et al.*, 2008; *Znachor et al.*, 2013]. Silicon retention is thus the net result of the interactions between the external supply of reactive Si, in-reservoir formation of biogenic silica, plus the dissolution and ultimate preservation of particulate reactive Si [*Lauerwald et al.*, 2012; *Teodoru et al.*, 2006; *Van Cappellen*, 2003].

A number of recent studies have addressed global Si retention by river damming. *Beusen et al.* [2009] used the Global-NEWS-DSi model, in which dissolved Si retention is assumed to correlate with global trends in phosphorus and sediment retention. *Laruelle et al.* [2009] introduced a correction factor in their global Si box model to simulate increased reactive Si retention on the continents under various damming scenarios. *Harrison et al.* [2012] took a step further with the development of the Silica Retention in Reservoirs and Lakes (SiRReLa) model. The SiRReLA model was statistically calibrated using a data set of 12 lakes and 15 reservoirs.

Harrison and coworkers proposed that the effects of trophic status and hydraulic load on the particle settling velocity represent the primary factors modulating Si retention in reservoirs. As with the work of *Beusen et al.* [2009], the SiRReLa model only accounts for the retention of dissolved Si. More recently, *Frings et al.* [2014] derived an average accumulation rate of biogenic silica in reservoirs, based on data from 18 reservoirs. By multiplying this rate by the total reservoir surface area, they then computed the mass of reactive Si retained annually by dams. A major source of uncertainty in the work of both *Harrison et al.* [2012] and *Frings et al.* [2014] is the small size of the data sets on which the global estimates are based.

Here we reevaluate worldwide reactive Si retention by man-made river dams, by combining existing data on dissolved Si retention with a mechanistic model of biogeochemical Si cycling in reservoirs. The proposed approach is designed to compensate for the sparse data on Si budgets in artificial reservoirs. The process-based model accounts for the fate of both reactive dissolved and particulate Si in reservoir systems. The model is calibrated with existing data on dissolved Si retention in reservoirs, while a Monte Carlo analysis accounts for the effects of the statistical variability of reservoir characteristics on the model-predicted retention of reactive Si. Based on the results, we then derive a relationship between reactive Si retention and water residence time and use it to estimate global accumulation of reactive Si in reservoirs.

2. Terminology

In this paper, reactive Si (RSi) refers to the sum of dissolved reactive Si and reactive particulate Si. Dissolved reactive Si (DSi) consists almost entirely of monomeric silicic acid or silicon hydroxide (H_4SiO_4). In most freshwaters, ionized forms of silicic acid and silica dimers and polymers only contribute minute fractions of DSi [*Iler*, 1979]. Reactive particulate Si (PSi) comprises all particle-associated Si that can potentially dissolve prior to removal by burial in bottom sediments or river outflow. The distinction between reactive and unreactive particulate Si is somewhat subjective and depends on the reservoir under consideration. The input of PSi to a reservoir includes soil- and river-derived amorphous silica (SiO_2) and hydrous, poorly crystalline aluminosilicates, as well as Si sorbed to minerals, for example, ferric oxyhydroxides [*Davis et al.*, 2002], and natural organic matter. For many reservoirs, the PSi input likely consists largely of biogenically produced SiO_2, that is, structural siliceous deposits produced by plants (phytoliths), diatoms, and other organisms [*Saccone et al.*, 2007; *Sauer et al.*, 2006; *Teodoru et al.*, 2006; *Van Cappellen*, 2003]. Production of siliceous frustules by diatoms within the reservoir or lake further adds to the PSi pool.

Retention of RSi refers to its removal by processes in the reservoir. The main sink for RSi is burial of PSi in bottom sediments. Because data on PSi burial fluxes in artificial reservoirs are fairly scarce [*Frings et al.*, 2014], RSi retention is generally estimated from the difference between measured input and output fluxes:

$$R_R = \frac{\mathrm{RSi_{in}} - \mathrm{RSi_{out}}}{\mathrm{RSi_{in}}} \quad (1)$$

where R_R is the relative retention of RSi (unitless), and $\mathrm{RSi_{in}}$, and $\mathrm{RSi_{out}}$ are the input and output fluxes of reactive Si in units of mass per unit time. Equation (1) assumes that, on an annual basis, the reservoir's RSi budget is close to steady state. In most studies, the inputs and outputs of reactive Si are assumed to occur entirely via the river network, hence neglecting potential contributions to the RSi budget by atmospheric deposition or groundwater flow.

Because data sets on Si budgets for reservoirs usually only include measurements of DSi, but not PSi, usually only the retention of DSi is calculated from

$$R_D = \frac{\mathrm{DSi_{in}} - \mathrm{DSi_{out}}}{\mathrm{DSi_{in}}} \quad (2)$$

where R_D is the relative retention of DSi (unitless), and $\mathrm{DSi_{in}}$ and $\mathrm{DSi_{out}}$ are the input and output fluxes of DSi. The values of R_D and R_R converge when DSi dominates RSi inputs and outputs. The latter is in fact an implicit assumption in most existing studies on Si retention in reservoirs and lakes. The input of $\mathrm{DSi_{in}}$ is typically calculated as the product of inflow discharge (Q_{in}) and the inflow DSi concentration (C_{in}). In reservoirs that discharge all water through the dam (e.g., hydroelectric reservoirs), $\mathrm{DSi_{out}}$ is similarly the product of outflow discharge (Q_{out}) and outflow DSi concentration (C_{out}). For storage reservoirs (e.g., reservoirs used for irrigation or municipal water supply), $\mathrm{DSi_{out}}$ is split between the water flow pumped out of the reservoir and that discharged through the dam. In order to maintain a water balance, the sum of the water flows pumped out of

the reservoir and discharged through the dam is assumed to equal Q_{in}; that is, losses through groundwater recharge and evaporation are neglected. Unless available information indicates otherwise, we assume that the DSi concentrations in the pumped and discharged water flows are the same. In what follows, water fluxes, concentrations, and retentions refer to annual averages.

3. Data Set

An exhaustive literature search yielded only 20 reservoirs for which R_D was provided or could be estimated (Table 1). (Note that we focus on DSi retention, because of the general lack of PSi measurements.) For comparative purposes, a data set of 24 natural lakes was also assembled (Table S1 in supporting information). The reservoir data set in Table 1 extends those of *Harrison et al*. [2012] and *Frings et al*. [2014]. We only included artificial reservoirs associated with constructed dams. Thus, causeways, such as Lake Lugano, and natural impoundments, such as Lake Pepin, were not considered as reservoirs. For each reservoir or lake, the following information was collected: (1) surface area, (2) volume, (3) average water depth, (4) river discharge, (5) hydraulic load, (6) annual DSi influx and (7) efflux, (8) water residence time, (9) trophic status, (10) bedrock lithology of the catchment, (11) pH, and (12) climate (that is, temperature and precipitation). In addition, for the reservoirs we included the (13) primary function and (14) age of the reservoir.

The effects on DSi retention of the reservoir and lake properties included in the database were assessed through analysis of variance, *t* tests, and regression models. The statistical analyses aimed at identifying the key variables to be included in the mechanistic Si reservoir model (section 4). A complete description of the results of the statistical analyses can be found in Appendix S1 and Table S2 in the supporting information. Local bedrock lithology was obtained from the various countries' national geological maps and crosschecked against the global lithology map (GLiM) database [*Hartmann and Moosdorf*, 2012]. Water residence time (τ_r) was calculated as $\tau_r = V/Q_{in}$, where V is the lake or reservoir volume and Q_{in} the combined river inflow. In the absence of information on trophic status, or when it was poorly supported, we relied on *Carlson and Simpson*'s [1996] trophic status index approach. When not stated in the reference(s) listed in Table 1, the primary reservoir function (e.g., hydroelectricity production, irrigation, drinking water supply, or other) was extracted from the Global Reservoirs and Dams (GRanD) database [*Lehner et al*., 2011]. Average annual precipitation and temperature were obtained for the nearest town or city from the *World Climate* [2005] database and Environment Canada for Canadian lakes; for Toolik Lake, Alaska, climate data were retrieved from the Toolik Field Station website (http://toolik.alaska.edu/). The age of a reservoir is the number of years between dam closure and the date of data collection as stated in the original literature source. In those cases where data covered a range of years (e.g., Lake Alexandrina), the midpoint age was used. The age reported for the recently completed Suofenying Reservoir is "0 years" [*Wang et al*., 2010]. In order to include this reservoir in the statistical analyses, we arbitrarily assigned a reservoir age of 0.1 years.

While originally data for 22 reservoirs were found, detailed analysis of the literature sources revealed that in a few of the studies major river inflows to the reservoir were neglected, thus introducing significant uncertainty in the estimated DSi retention. The most notable examples are Amistad Reservoir and the Lower Columbia Basin, for which the available data yielded large negative DSi retentions (-0.2 and -0.67, respectively). These reservoirs were all together removed from further analysis. Additionally, three reservoirs (Ardleigh, Suofenying, and Masinga) were excluded from the mechanistic model calibration (for justifications, see caption of Table 1). Thus, in total, 20 reservoirs were included in the statistical tests and 17 reservoirs in the calibration of the mechanistic model.

Comparison of the 20 reservoirs in Table 1 to the Global Reservoirs and Dams (GRanD) database [*Lehner et al*., 2011] (Figure 1) reveals a lack of reservoirs in Table 1 with water residence times over 3 years, which account for 21% of the GRanD reservoirs. They further point to a possible bias of our data set toward reservoirs in areas dominated by limestone and, thus, toward more alkaline pH, which may increase the dissolution and decrease the preservation of biogenic silica [*Van Cappellen and Qiu*, 1997; *Ryves et al*., 2006]. Our data set provides a reasonably good climatic distribution, with the majority of reservoirs located in temperate and subtropical latitudes, although no DSi retentions were obtained for arctic and subarctic reservoirs, which account for 8% of the GRanD reservoirs. All major reservoir functions, particularly, hydroelectricity generation and flood control, are represented in Table 1.

A key outcome of the statistical analyses is that R_D significantly differs between reservoirs and lakes ($p < 0.0001$) with, on average, 42% more DSi retention in lakes compared to reservoirs. In addition, reservoirs typically

Global Biogeochemical Cycles

10.1002/2014GB004875

Table 1. Reservoir Data Set: See Text for Details

Latitude	Reservoir Name	Location	Bedrock Lithology	Trophic Status	Surface Area (km^2)	Mean Depth (m)	pH	Climate	Residence Time (years)	DSi Influx ($mol\,yr^{-1}$)	R_D	Primary Usage	Age (years)	References[a]
26.97	Suofenying[b]	China	Carbonate	Meso	5.7	23.5	8.06	Subtropical	0.016	4.56×10^{8}	−0.072	Hydroelectric	0	1
26.9	Dongfeng	China	Carbonate	Oligo	19.7	52	8.06	Subtropical	0.1	3.99×10^{8}	−0.055	Hydroelectric	12	1
27.3	Wujiangdu	China	Carbonate	Eu	47.5	48.4	8.06	Subtropical	0.14	5.41×10^{8}	0.23	Hydroelectric	27	1
36.9	Lake Powell	USA	Sandstone	Oligo	658	40	8.5	Subtropical	2.3	4.81×10^{9}	0.081	Irrigation	29	2
36.4	Lake Mead	USA	Sandstone	Meso	640	40	8.3	Subtropical	2.6	4.94×10^{9}	0.13	Irrigation	62	2, 21
26.6	Falcon	USA	Mixed sedimentary	Eu	338.5	11.52	7.9	Subtropical	1	7.02×10^{8}	0.17	Irrigation	44	2
44.6	Iron Gate	Romania	Mixed sedimentary, carbonate	Eu	156.4	17.3	8.0	Temperate	0.03	1.41×10^{10}	0.040	Hydroelectric	29	3, 4, 5
48.2	Amance	France	Carbonate	Eu	0.5	4.5	N/A	Temperate	0.03	5.39×10^{7}	0.089	Flood control	4	6
48.2	Seine	France	Carbonate	Eu	23	7.6	N/A	Temperate	0.62	5.45×10^{7}	0.43	Flood control	28	6, 7
48.2	Aube	France	Carbonate	Eu	21	8.9	N/A	Temperate	0.4	2.32×10^{7}	0.57	Flood control	4	6
48.3	Marne	France	Carbonate	Eu	48	7.2	N/A	Temperate	0.46	5.39×10^{7}	0.48	Flood control	20	6
48.3	Champaubert	France	Carbonate	Eu	0.5	3.5	N/A	Temperate	0.11	2.32×10^{7}	0.158	Flood control	20	6
21.7	Thac Ba	Vietnam	Gneiss, carbonate	Meso	235	58	7.5	Tropical	2.2	7.19×10^{9}	0.012	Hydroelectric	31	8, 9
20.5	Hoa Binh	Vietnam	Mixed sedimentary, carbonate	Meso	208	46	5.57	Tropical	0.09	8.07×10^{9}	0.16	Hydroelectric	9	8, 9, 20
30.8	Three Gorges	China	Carbonate	Eu	1100	35.5	8.04	Subtropical	0.097	4.65×10^{10}	0.038	Hydroelectric	4	10, 11
−6.9	Saguling	Indonesia	Volcanic	Eu	56	18.4	7.6	Tropical	0.23	1.49×10^{9}	0.382	Hydroelectric	18	13
−0.9	Masinga[b]	Kenya	Mixed igneous/ metamorphic	Meso	120	13.3	8.2	Tropical	0.25	N/A	0.4	Hydroelectric	27	14
−35.5	Lake Alexandrina	Australia	Carbonate	Eu	580.6	2.86	8.6	Subtropical	0.3	9.29×10^{8}	0.39	Irrigation	47.5	15, 16, 17
51.5	Ardleigh[b]	England	Mixed sedimentary	Eu	0.57	3.8	8.2–9.4	Temperate	0.36	1.39×10^{6}	0.79	Water supply	13	18
49.2	Solina-Myczowce	Poland	Mixed sedimentary	Meso	24	22	6.4–6.8	Temperate	0.61	3.25×10^{7}	0.20	Hydroelectric	36	19

[a]References: (1) *Wang et al.* [2010]; (2) *Kelly* [2001]; (3) *Teodoru and Wehrli* [2005]; (4) *Friedl et al.* [2004]; (5) *McGinnis et al.* [2006]; (6) *Garnier et al.* [1999]; (7) *Thieu et al.* [2009]; (8) *Le Thi Phuong et al.* [2010]; (9) *Nam* [1995]; (10) *Müller et al.* [2012]; (11) *Ran et al.* [2013]; (13) *Husnain and Masunaga* [2009]; (14) *Hughes et al.* [2012]; (15) *Cook et al.* [2010]; (16) *Geddes* [1984]; (17) *Mosley et al.* [2012]; (18) *Redshaw et al.* [1988]; (19) *Koszelnik and Tomaszek* [2008]; (20) *Interim Scientific Advisory Group* [2000]; (21) *Hoffman et al.* [1967].

[b]Indicates reservoirs excluded from the calibration of the mechanistic model but included in the statistical analyses (Ardleigh's water budget was unbalanced, Masinga was missing DSi flux information, and initial conditions for Suofenying could not be reconstructed).

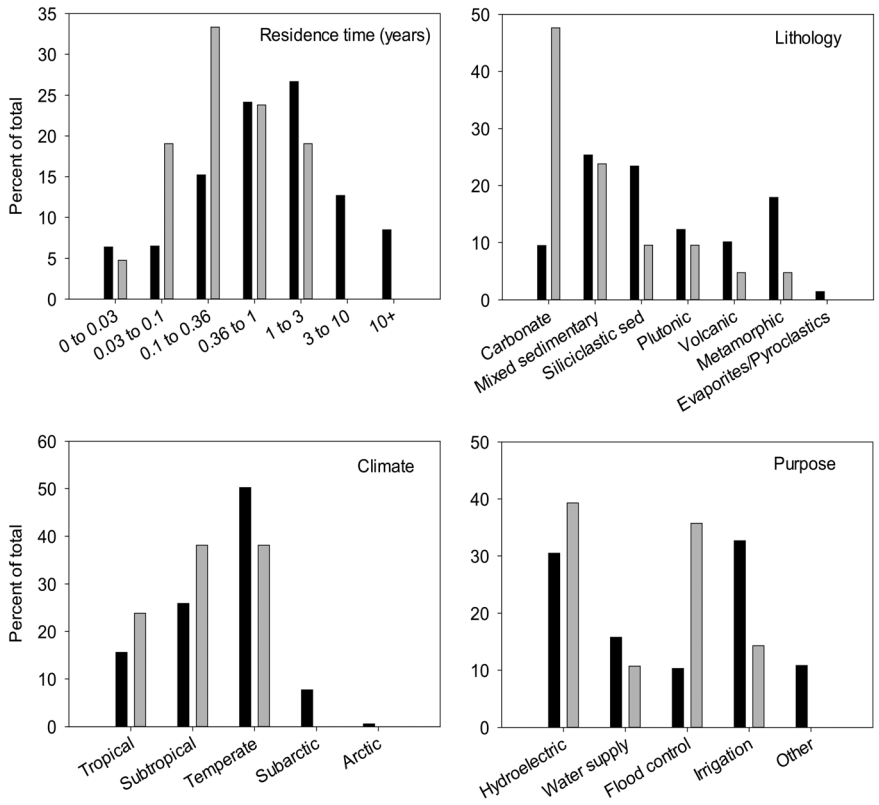

Figure 1. Comparison of reservoirs included in the calibration data set (gray bars), described in section 3 and Table 1, and those of the GRanD database (black bars), according to residence time (in units of years), bedrock lithology, climate, and reservoir purpose. "Other" reservoir purposes include fisheries, navigation, and recreation.

exhibit lower water residence times (τ_r) and higher hydraulic loads than lakes. The statistical analyses further imply that grouping lakes and reservoirs together may generate spurious results. For example, when combining lakes and reservoirs, a significant ($p < 0.05$) dependence of R_D on the catchment lithology is found, with metamorphic and crystalline felsic rocks yielding the highest DSi retention and carbonate rocks the lowest. However, when lakes are removed from the data set, the trend is no longer apparent, suggesting that the relationship between R_D and lithology may be representative of lakes, but not of reservoirs. Reactive Si cycling in reservoirs is thus statistically distinct from that in lakes, which argues against merging data from both types of systems into a single data set when estimating global lentic Si retention, as done by *Harrison et al.* [2012]. Therefore, in what follows, only the data from the artificial reservoirs are considered. The nonlinear regressions further imply that, for reservoirs, R_D is most closely related to τ_r.

Although the 20 reservoirs in Table 1 encompass a fairly broad range of settings and reservoir characteristics, as can be seen in Figure 1, it is important to emphasize that they represent less than 0.03% of the more than 75,000 reservoirs with a surface area ≥0.1 km^2 [*Lehner et al.*, 2011]. The limited data set is thus unlikely to be statistically representative of reservoirs worldwide. For this reason, the primary function of the data set is to calibrate a mechanistic model of Si cycling in reservoirs, which incorporates well-understood processes and parameter values constrained through an extensive literature review. The model then provides the means to extrapolate the sparse data set to the global scale.

4. Mechanistic Si Cycling Model

4.1. Model Description

A four-box biogeochemical model is used to simulate annual reactive Si (RSi) cycling in reservoirs (Figure 2). In the model, the inputs to and outputs from the reservoir occur under the form of both reactive particulate (PSi) and dissolved silica (DSi). Note that the model does not distinguish between different input and output

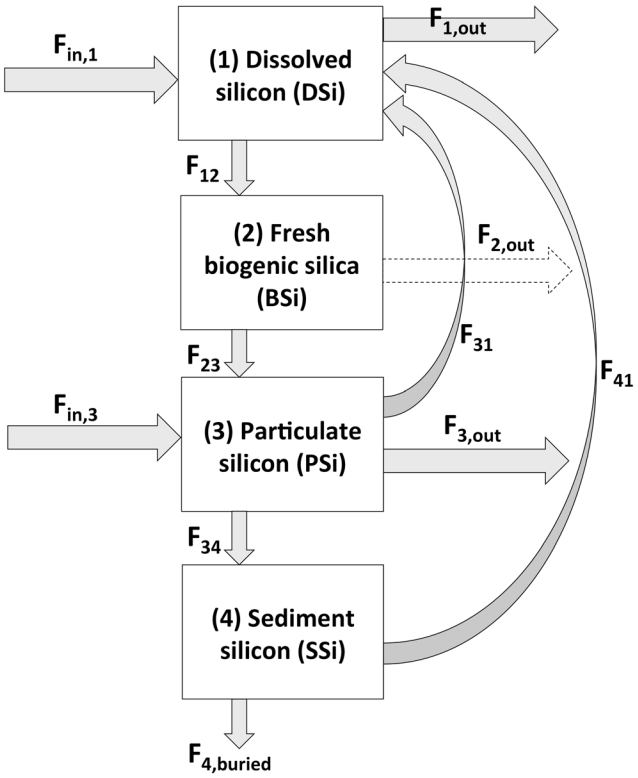

Figure 2. Mechanistic model of biogeochemical silicon cycling in reservoirs. See text for details.

pathways. Thus, the input flux of DSi for instance includes river inflow as well as potential contributions by atmospheric deposition and groundwater discharge. Within the reservoir, dissolution of PSi generates additional DSi, while siliceous organisms, primarily diatoms, transform DSi into biogenic silica (BSi). The BSi pool represents silica deposits within living or recently deceased biomass, that is, silica still surrounded by protective organic membranes. Upon the degradation of the organic membranes, BSi integrates into the PSi pool and is, from then on, exposed to dissolution [*Loucaides et al*., 2012]. The PSi that does not dissolve is exported downstream or accumulates in the sediments. In order to account for the fairly rapid loss in reactivity of particulate Si (i.e., aging), as well as the buildup of pore water DSi, the sediment Si pool (SSi) was assigned a much lower rate constant of dissolution than PSi [*Van Cappellen et al*., 2002]. The fraction of SSi that escapes dissolution is permanently removed by burial in the reservoir's sediments.

The annual input fluxes of DSi and PSi to the reservoir were imposed in the model. As a default value, we assumed that the PSi influx was equal to 10% of the DSi influx, based on the global estimate of riverine PSi by *Conley* [1997] and supported by data of *Ran et al*. [2013] and *Triplett et al*. [2012]. With one exception, all internal and outflow fluxes were assigned first-order rate expressions with respect to the source reservoirs [*Laruelle et al*., 2009]. The exception was siliceous productivity, F_{12}, which was calculated assuming parabolic saturation kinetics [*Valiela*, 1995]:

$$F_{12} = \frac{R_{\max} \times [\mathrm{DSi}]}{K_s + [\mathrm{DSi}]} \tag{3}$$

where $R_{\max}$ is the maximum rate of BSi production, [DSi] the DSi concentration, and K_s the half-saturation constant for DSi uptake by siliceous organisms. The value of $R_{\max}$ represents the reservoir's mean annual carrying capacity for biological Si fixation.

In the model, the reservoir is treated as a well-mixed reactor; the rate constants for the outflow fluxes of DSi and PSi (i.e., $F_{1,\mathrm{out}}$ and $F_{3,\mathrm{out}}$) are therefore equal to the inverse of the water residence time. Default values for the other linear rate constants and for K_s were derived from in-depth reviews of the literature (Table 2). The values of $R_{\max}$ are reservoir specific and determined as explained in the next section. The mass balance equations were solved in MATLAB for time steps of 0.01 year using Runge-Kutta 4 integration. Reservoir age was incorporated by running the models for the number of years since river damming; e.g., for a 20 year old reservoir, the model was run for 2000 time steps.

The mechanistic model provides a highly simplified description of Si cycling, in line with the sparse database on reactive Si budgets for reservoirs. Some processes are not included, for example, the direct incorporation of DSi into the SSi pool via clay mineral formation, while other processes are merged into a single flux. For instance, the fluxes F_{23} and F_{34} on Figure 2 combine reactive silica transformations and vertical transport. In addition, the model does not resolve seasonal effects on Si cycling in reservoirs, such as diatom blooms, flow variability, or water column stratification. The model thus represents a first step in the knowledge-based scaling up of the limited data on Si dynamics in reservoirs.

Table 2. Fluxes and Parameters of the Mechanistic Si Reservoir Model (Figure 2)[a]

	Flux	Default Value	Range	Reference
$F_{in,1}$	DSi influx	Reservoir specific	2.32×10^{7}–4.65×10^{10} mol yr^{-1}	See Table 1
$F_{in,3}$	PSi influx	10% of DSi influx	0–54% DSi influx	*Ran et al.* [2013], *Triplett et al.* [2012], *Conley* [1997], and *Harrison et al.* [2012]
F_{12}	Biological DSi uptake	R_{max} = calculated using equation (4). K_s = 0.005 mol m^{-2}	R_{max}: see Table 3 K_s: 5×10^{-7}–0.05 mol m^{-2}	*Van Donk and Kilham* [1990], *Michel et al.* [2006], *Znachor et al.* [2013], and *Brzezinski et al.* [1997]
F_{31}	Fresh PSi dissolution	k_{31} = 3 yr^{-1}	0.2–40 yr^{-1}	*Van Cappellen et al.* [2002] and *Loucaides et al.* [2012]
F_{23}	Decay siliceous biomass	k_{23} = 25 yr^{-1}	5–250 yr^{-1}	*Dai et al.* [2009] and *Wetz et al.* [2008]
F_{34}	PSi aging plus sedimentation	k_{34} = 10 yr^{-1}	5–45 yr^{-1}	*Horn and Horn* [2000]
$F_{1,out}$	DSi efflux from reservoir	$k_{out}=1/\tau_n$ where τ_r is residence time in years.	$F_{1,out}$:1×10^{7}–4.47×10^{10} mol yr^{-1}	See Table 1; volume data from *Lehner et al.* [2011]
$F_{3,out}$	PSi efflux from reservoir	$k_{out}=1/\tau_r$	Same as above	Same as above
F_{41}	Dissolution deposited SSi	k_{41} = 0.01 yr^{-1}	0.002–0.16 yr^{-1}	*Van Cappellen et al.* [2002] and *Loucaides et al.* [2012]
$F_{4,buried}$	Permanent burial SSi	$k_{4,buried}$ = 0.002 yr^{-1}	NA	*Laruelle et al.* [2009]

[a]Details on the fluxes and assumptions are given in the text (section 4). Ranges are compiled from diverse literature sources.

4.2. Siliceous Production: Calibration

The mass balance Si model was applied to the 17 reservoirs of the calibration data set described in section 3. For each reservoir the corresponding river discharge, reservoir volume, water residence time (τ_r), DSi influx and age (i.e., years since dam closure) were imposed. After assigning the default parameter values of Table 2, the only remaining free model parameter was the maximum siliceous production rate, R_{max}. For each of the reservoirs, the value of R_{max} was adjusted until the calculated DSi retention, R_D, matched the observed value.

The model-derived R_{max} values fall between 0.5 and 14.7 mol Si m^{-2} yr^{-1} (Table 3), that is, values consistent with observed diatomaceous production rates. Reservoirs receiving inflow with low DSi concentrations (15–70 μM, Dongfeng, Marne, Aube and Solina reservoirs) exhibit R_{max} values comparable to mean open ocean diatom productivities (0.6–0.8 mol Si m^{-2} yr^{-1}) [*Nelson et al.*, 1995; *Krause et al.*, 2011]. The other model-derived R_{max} values are similar to silicon uptake rates measured in lakes and reservoirs. For example, siliceous productivities reported for Lake Michigan, Lake Ontario, Lake Superior, Lake Myvatn (Iceland), and two natural impoundments on the Mississippi River (Pepin and St. Croix) range from 0.5 to 7.1 mol Si m^{-2} yr^{-1} [*Schelske*, 1985; *Opfergelt et al.*, 2011; *Triplett et al.*, 2008], while for the Three Gorges Reservoir they fall between 1.6 and 2.7 mol Si m^{-2} yr^{-1} [*Ran et al.*, 2013]. The highest R_{max} values (≥10 mol Si m^{-2} yr^{-1}, Amance, Champaubert, and Saguling reservoirs) are within the range of siliceous productivities measured in coastal upwelling areas, where values can be as high as 416 mol Si m^{-2} yr^{-1} [*Nelson et al.*, 1995; *Brzezinski et al.*, 1997].

Table 3. Maximum Siliceous Primary Productivity (R_{max}) and Predicted RSi Retention (R_R) for Reservoirs in the Data Set[a]

Reservoir	R_{max} (mol m^{-2} yr^{-1})	Predicted R_R
Iron Gate	5.43	0.02
Amance	11.40	0.04
Hoa Binh	8.27	0.11
Lake Alexandrina	1.16	0.29
Dongfeng	0.51	0.04
Champaubert	10.60	0.11
Wujiangdu	4.00	0.15
Saguling	14.73	0.29
Aube	0.84	0.48
Marne	0.84	0.41
Solina-Myczowce	0.54	0.22
Seine	1.74	0.40
Falcon	0.81	0.21
Thac Ba	2.87	0.10
Lake Powell	1.45	0.16
Lake Mead	3.13	0.19
Three Gorges	2.64	0.06

[a]See text for detailed discussion.

Nonlinear regression indicates that the R_{max} values most strongly correlate with the input fluxes of DSi into the reservoirs. The following power relationship predicts R_{max} across more than 3 orders of magnitude (Figure 3):

$$R_{max} = 10.837 \times DSi_{in}^{\,0.8126} \quad (R^2 = 0.83) \qquad (4)$$

where R_{max} and DSi_{in} are both given in mol yr^{-1}. (Note that the R_{max} values in Table 3 are converted to units of mol yr^{-1} through multiplication with

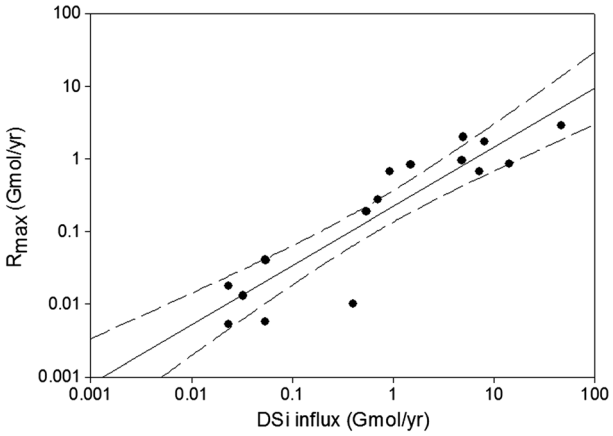

Figure 3. Maximum siliceous productivity, R_{max}, for the 17 reservoirs used to calibrate the mechanistic model, plotted against the DSi input. The solid line corresponds to equation (4). Dashed lines are 95% confidence intervals. The R_{max} values are listed in Table 3.

the corresponding reservoir surface areas given in Table 1.) A positive correlation between R_{max} and DSi_{in} is not surprising: the higher the supply of bioavailable Si to a reservoir, the more siliceous production can be sustained. Other factors are expected to affect R_{max}, however. These include temperature, light intensity, turbidity, the availability of other essential nutrients, such as phosphorus and nitrogen, and reservoir hydrodynamics. These factors may in part explain the scatter seen in Figure 3.

4.3. Sensitivity Analyses

In order to analyze parameter sensitivity of the mechanistic model, we defined the following hypothetical, average reservoir, based on the information in Table 1. The reservoir is 10 years old and has a volume of 6 km^3, a surface area of 210 km^2, and a river discharge of 35 $km^3\,yr^{-1}$ (i.e., $\tau_r = 0.17$ years). The inflow to the reservoir was assigned the global average river DSi concentration of 162.5 μM, according to the GloRiCh database of world river nutrient concentrations (J. Hartmann, University of Hamburg, personal communication, 2013). From equation (4), an R_{max} value of 6.0×10^8 mol yr^{-1} was obtained. All other parameters were assigned the default values listed in Table 2. Parameter values were then doubled and halved in turn, and the effects on the predicted R_D and R_R values were quantified. The results of the sensitivity analysis are summarized in Table S3 (supporting information). They reveal that R_{max} is the most sensitive parameter governing the model-predicted values of R_D and R_R. Doubling (halving) R_{max} yields a percent increase (decrease) of R_D by 68% (138%). Thus, not unexpectedly, RSi retention in reservoirs is highly sensitive to biological Si fixation.

In the above example, the computed DSi and RSi retentions are not sensitive to the age of the reservoir in the range tested (5–20 years). The latter range, however, far exceeds the water residence time of the reservoir (0.17 years). In fact, right after dam closure, R_D and R_R are quite sensitive to the age of the reservoir (Figure 4). When sediment starts to accumulate, retention of reactive Si is initially relatively high. As the sediment builds up, dissolution of the SSi pool returns increasing amounts of DSi to the water column, hence causing R_D and R_R to decrease. After about 1.5 years, the R_D and R_R values stabilize. (Note that for reservoirs with longer water residence times, it takes longer for R_D and R_R to stabilize).

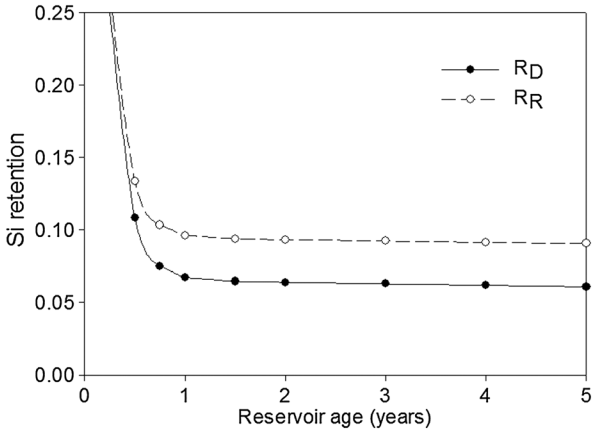

Figure 4. Retentions of DSi and RSi as a function of reservoir age, for the hypothetical "average" reservoir defined in section 4.3.

4.4. Monte Carlo Analysis

The statistical and sensitivity analyses imply that RSi retention by river damming is most strongly related to reservoir hydraulics and siliceous productivity. To account for the large variability in these reservoir characteristics, a Monte Carlo analysis of the mechanistic Si cycling model was performed by randomly varying the following variables within prescribed ranges: (1) volume (0.001–180 km^3), (2) reservoir age (0.5–100 years), (3) discharge (0.01–40 $km^3\,yr^{-1}$), (4) DSi inflow concentration (30–1500 μM), (5) PSi influx (0.5–30% of DSi influx), and (6) R_{max} (equation (4) ± 1 order of magnitude).

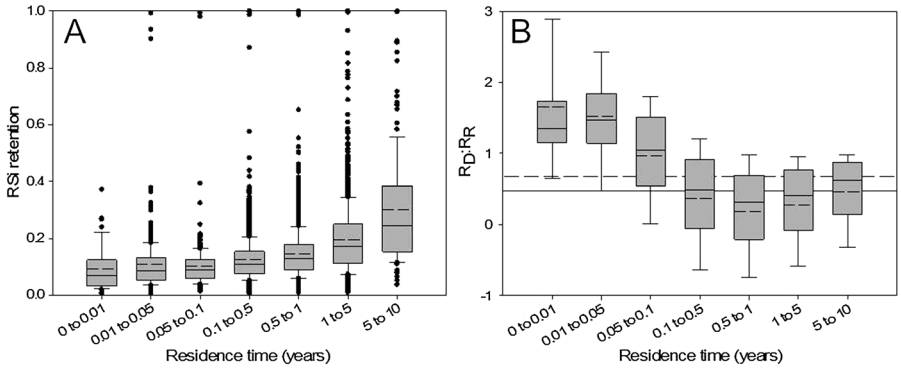

Figure 5. Monte Carlo analysis of mechanistic model: (a) RSi retention (R_R) values for 6000 model realizations versus the water residence time and (b) R_D:R_R ratios for the same 6000 model realizations versus the water residence time. The dashed horizontal line in Figure 5b corresponds to the (arithmetic) mean R_D:R_R ratio (0.65) and the solid horizontal line to the globally weighted R_D:R_R ratio (0.45). See text for more details. Inside each box on both panels, the solid line indicates the median, the dashed line the mean value. The edges of each box represent the first and third quartiles, and the whiskers are standard deviations. Note that outliers are not shown in Figure 5b.

The above ranges were selected based on reported values in the literature, excluding obvious outliers. Only variables for which parameter ranges could be quantitatively constrained were included in the Monte Carlo analysis. The variables were further assumed to vary independently from one another, although some of the variables may be weakly correlated. Once the values of reservoir volume and discharge were selected, the water residence time was calculated as $\tau_r = V/Q_{in}$. The simulations further allowed for the possibility of BSi export from the reservoir via the dam outflow. (Note that in the baseline version of the model, only DSi and PSi are exported from the reservoir.) The BSi efflux was calculated by multiplying the BSi concentration with the inverse of the water residence time (as for the DSi and PSi effluxes) and a randomly generated coefficient ranging from 0 to 1. All other model parameters were assigned their default values listed in Table 2. The analysis was carried out on 6000 model realizations.

The results of the Monte Carlo analysis are illustrated in Figure 5. As expected, for any given water residence time the computed total reactive Si retention, R_R, values cover a wide range (Figure 5a). The outlying values typically correspond to combinations of extreme reservoir characteristics. For example, R_R values approaching 1 at the lower residence times are primarily associated with very small reservoirs exhibiting extremely high productivities (i.e., much higher than predicted with equation (4)). Overall, most R_R values tend to fall between 0.03 and 0.5, with average values increasing with increasing water residence time.

The Monte Carlo analysis further reveals a systematic variation of the relative contributions of dissolved and particulate Si to total reactive Si retention, with increasing water residence time (Figure 5b). Short residence times result in a more efficient downstream export of PSi produced by in-reservoir siliceous production. Hence, at low τ_r, reactive Si retention tends to be dominated by the removal of inflowing DSi. As τ_r increases, however, there is more time for the PSi and SSi pools to dissolve back to DSi. The relative contribution of R_D to the total retention of reactive Si then decreases, as seen for the model-predicted average R_D: R_R ratios (Figure 5b).

The general trend of R_R with respect to the water residence time was fitted to various standard curves (Figure S1 in the supporting information). The following power law relationship yields the best fit:

$$R_R = 0.1746 \times \tau_r^{0.2973} \quad \left(R^2 = 0.31,\ p < 0.0001\right) \tag{5}$$

where τ_r is expressed in units of years. For consistency, a similar power law equation is fitted to the DSi retention values generated by the Monte Carlo simulations:

$$R_D = 0.0938 \times \tau_r^{0.4066} \quad \left(R^2 = 0.12,\ p < 0.0001\right) \tag{6}$$

(Note that the R_D values are shown in Figure S2 in the supporting information.)

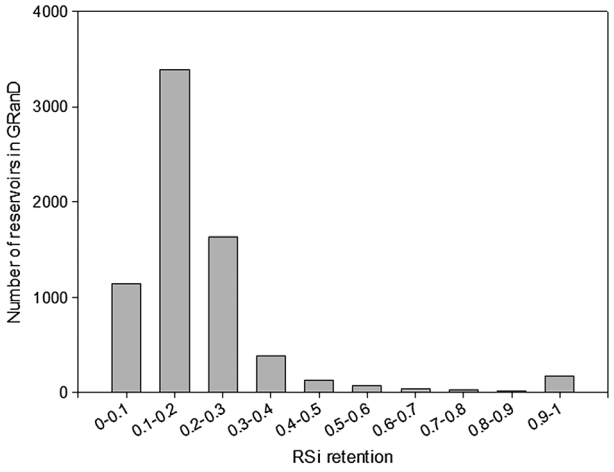

Figure 6. Distribution of model-derived RSi values for the reservoirs of the GRanD database. Arithmetic mean = 0.20, median = 0.17, and standard deviation = 0.16.

5. Global Si Retention by River Damming

5.1. Approach

The estimation of the global retentions of RSi and DSi by river damming assumes that equations (5) and (6) offer a reliable representation of reactive Si dynamics in reservoirs. We emphasize that the equations are not necessarily good predictors for any specific individual reservoir, but rather that they provide a meaningful representation of the average behavior of Si when considering a large ensemble of reservoirs. The equations are then applied to the Global Reservoirs and Dams (GRanD) database [*Lehner et al*., 2011], which comprises information on 6862 reservoirs and their associated dams. Note that the previous global estimate of DSi retention in reservoirs by *Harrison et al*. [2012] was based on the earlier, smaller subset of 822 reservoirs presented by *Lehner and Döll* [2004]. The GRanD database classifies several natural lakes as reservoirs if they are used as a primary water supply (e.g., Lake Ontario and Lake Victoria). In order to ensure that no natural lakes are included in the estimates given below, the GRanD database was overlain with Lehner and Döll's Global Lakes and Wetlands Databases levels 1 and 2 (large and small lakes). Water bodies appearing in both data sets were removed from the calculations.

For each reservoir, the DSi input from the corresponding watershed was obtained from the Global-NEWS-DSi model, using the predam scenario [*Beusen et al*., 2009]:

$$\mathrm{DSi_{in}} = W \times \mathrm{SiY} \tag{7}$$

where $\mathrm{DSi_{in}}$ is given in units of mol $\mathrm{yr^{-1}}$, W is the upstream watershed area ($\mathrm{km^2}$) listed in the GRanD database, and SiY is the DSi yield of the watershed in units of mol Si $\mathrm{km^{-2}\,yr^{-1}}$. Equation (7) assumes a uniform DSi yield throughout a given catchment [*Hartmann et al*., 2009; *Jansen et al*., 2010; *Harrison et al*., 2012]. The amount of DSi retained annually in the reservoir was then obtained as (see equation (2)):

$$\mathrm{DSi_{ret}} = \mathrm{DSi_{in}} - \mathrm{DSi_{out}} = R_D \times \mathrm{DSi_{in}} \tag{8}$$

where R_D was calculated with equation (6). Because Global-NEWS only provides DSi yields, it was assumed that, globally, the river supply of PSi equals 10% of that of DSi (see above). Thus, the amount of reactive silica retained annually in a reservoir was computed as follows:

$$\mathrm{RSi_{ret}} = \mathrm{RSi_{in}} - \mathrm{RSi_{out}} = R_R \times 1.1 \times \mathrm{DSi_{in}} \tag{9}$$

where R_R was calculated using equation (5) and the 1.1 factor accounts for the 10% reactive PSi input. The water residence time used in equations (5) and (6) was derived from the discharge and volume given in GRanD.

The frequency distribution of the R_R values calculated with equation (5) for the GRanD reservoirs is shown in Figure 6. The distribution shows a positive skew toward lower retentions, with over 3000 reservoirs with RSi retentions between 0.1 and 0.2, followed by about 1600 reservoirs with retentions between 0.2 and 0.3. The arithmetic mean for R_R value is 0.20 and that for R_D is 0.13. The mean R_D:R_R ratio (0.13:020 = 0.65) is plotted as the solid horizontal line in Figure 5b. As can be seen, reservoirs with water residence times less than 0.1 year tend to have R_D:R_R ratios exceeding the mean value, while the opposite is true for reservoirs with water residence times larger than 0.1 year.

The GRanD database accounts for at least 76% of the estimated global volume of reservoirs worldwide, with the bulk of the remaining 24% volume mainly including reservoirs less than 1 $\mathrm{km^2}$ in size [*Lehner et al*., 2011]. The latter are typically associated with low RSi retentions (Figure 5a). If we assume that the reservoirs not included in the GRanD database receive on the order of 24% of the global RSi input and exhibit, on average, only half the retention efficiency of the GRanD reservoirs (i.e., 10% rather than 20%,), then the missing reservoirs account for

Table 4. Output of Global Silica Retention Model

Description	Value
DSi retention (Gmol yr^{-1})	163.5
DSi retention (Tg SiO_2 yr^{-1})	9.79
DSi retention rate (mol m^{-2} yr^{-1})	0.44
Global average R_D (arithmetic)	0.13
RSi retention (Gmol yr^{-1})	372
RSi retention (Tg SiO_2 yr^{-1})	22.29
RSi retention rate (mol m^{-2} yr^{-1})	0.99
Global average R_R (arithmetic)	0.20
Siliceous productivity (Gmol yr^{-1})	516
Siliceous productivity (mol m^{-2} yr^{-1})	1.4
Recycling efficiency (%)	62

[a]Global reservoir surface area = 3.7×10^5 km^2 [*Lehner et al.*, 2011].

12% of RSi retention by river damming. A 12% extra contribution was therefore added to the total RSi retention computed for the GRanD reservoirs.

5.2. Global Estimates

With the approach described in the previous section, global RSi and DSi retentions in reservoirs are estimated to be equal to 372 Gmol yr^{-1} (22.3 Tg SiO_2 yr^{-1}) and 163 Gmol yr^{-1} (9.8 Tg SiO_2 yr^{-1}), respectively (Table 4). The Global-NEWS model yields a global DSi loading to watersheds of 6325 Gmol yr^{-1} for the predam scenario [*Beusen et al.*, 2009]. Assuming that PSi loading equals 10% that of DSi, a corresponding RSi loading of 6957 Gmol yr^{-1} is obtained. Thus, according to our estimates, 2.6% of the DSi and 5.3% of the RSi loadings to the world's river network are retained in dam reservoirs.

The 95% confidence interval of the power law for R_R as a function of water residence time (i.e., equation (5)) yields an error on the global RSi retention on the order of 1 Gmol yr^{-1}. This relatively small error indicates that the Monte Carlo analysis used to scale up the mechanistic model does not in itself introduce a large uncertainty on the global estimation of reactive Si retention. The main sources of uncertainty on the global estimates are associated with the calibration of the mechanistic model, the inputs of dissolved Si predicted by the Global-NEWS model, and the relative contribution of PSi to the total RSi input to reservoirs.

The globally weighted R_D:R_R ratio equals 0.45 (= 163/3001:372/3301), that is, a value markedly different from the mean R_D:R_R ratio (0.65 = 0.13:0.20). The reason is that global RSi retention is skewed toward reservoirs with higher water residence times, which, in turn, favor PSi retention (Figure 5b). Little data are available to confirm the dominant role of PSi in global reactive Si retention. To our knowledge, only the Si budgets for the Three Gorges Reservoir [*Ran et al.*, 2013], Lake St. Croix, and Lake Pepin [*Triplett et al.*, 2008] account for both DSi and PSi. For these three water bodies, the budgets imply that PSi retention exceeds DSi retention, in line with our global estimates.

Our estimated DSi retention is about one quarter lower than the global reservoir DSi retention of 516 Gmol yr^{-1} (31 Tg SiO_2 yr^{-1}) proposed by *Harrison et al.* [2012]. One major reason for the difference is that Harrison and coworkers used a combined data set including both lakes and reservoirs. Our analysis, however, shows that reservoirs are less efficient in retaining Si than lakes (section 3). Combining both lentic systems may thus lead to an overestimation of Si retention in reservoirs. In a recent study, *Frings et al.* [2014] derived PSi accumulation rates for 30 lakes and reservoirs from mass balance considerations. By multiplying the mean accumulation rate for the reservoirs only with the global reservoir surface area, these authors obtained a RSi retention of 230 Gmol yr^{-1}, that is, a value significantly lower than our estimate. The RSi retention proposed by Frings and coworkers, however, depends on the extent to which the average PSi accumulation rate of 18 reservoirs is representative of worldwide PSi retention in reservoirs.

With the mechanistic model presented in section 4 it is possible to make additional global-scale estimations. For example, application of the model to the GRanD database yields a global biological Si production in reservoirs of 516 Gmol yr^{-1}. Combined with the total surface area of reservoirs (3.7×10^5 km^2) [*Lehner et al.*, 2011], this translates into a mean siliceous productivity of 1.4 mol m^{-2} yr^{-1}. This value is higher than the average open ocean diatom productivity (0.6–0.8 mol m^{-2} yr^{-1}) [*Nelson et al.*, 1995] but similar to Si fixation in mesotrophic Lake Michigan (1.16 mol m^{-2} yr^{-1}) [*Schelske*, 1985]. Furthermore, according to the model, globally 62% of the external input plus in-reservoir production of PSi redissolves to DSi (Table 4). The latter estimate was obtained by calculating the reactive Si recycling efficiency (RE) for each of the reservoirs in the GRanD data set as follows:

$$\mathrm{RE} = \frac{F_{31} + F_{41}}{F_{\mathrm{in},3} + F_{12}} \times 100\% \tag{10}$$

The 62% estimate is of the same order of magnitude as reported Si recycling efficiencies for individual lakes and reservoirs, including 65% for Lough Neagh [*Dickson*, 1975; *Gibson et al.*, 2000], 66% for a dam reservoir on the Marne River [*Garnier et al.*, 1999], and 55% for the Three Gorges Reservoir [*Ran et al.*, 2013].

6. Conclusions

The global impact of dams on river Si fluxes is estimated via a new approach that merges biogeochemical modeling of reactive Si (RSi) cycling with data on reservoir Si budgets. A Monte Carlo analysis of the biogeochemical model yields a predictive relationship between reservoir RSi retention and water residence time, which, when applied to the GRanD data set, allows us to estimate global RSi retention by river damming. Although the construction of dams represents a major perturbation of the water cycle on the continents, the estimated retention of RSi in reservoirs is relatively small, on the order of 5% of the RSi loading to the world's river network. Nonetheless, with the global rise in phosphorus and nitrogen loadings to surface waters, even a small reduction in the worldwide riverine flux of RSi may exacerbate ecological changes that can lead to eutrophication of streams, lakes, and the coastal zone. The modeling results further imply that the building of dams may turn former river stretches into hot spots for siliceous productivity, fuelled by the efficient recycling of biogenic silica in reservoirs. By incorporating mechanistic knowledge of Si cycling, the proposed approach optimizes the extrapolation of the sparse data set on RSi retention in reservoirs to the global scale. Global retention in reservoirs of other nutrients, for example, phosphorus, could in principle be evaluated using a similar approach.

Acknowledgments

Additional data supporting statistical conclusions can be found in the supporting information, Table S1. To request access to the GIS files used in the global estimations, the computer codes for the mechanistic and Monte Carlo simulations, please contact Taylor Maavara at tmaavara@uwaterloo.ca. We thank Severin Stojanovic for help with the Monte Carlo analysis, Arthur Beusen (A.H.W.Beusen@uu.nl) for access to the complete Global-NEWS-DSi data set for the predam scenarios, and Jens Hartmann (jens.hartmann@zmaw.de) for sharing the GloRich database. Two anonymous reviewers provided valuable and constructive comments. We acknowledge S. Magdalene, Daniel Conley, and Patrick Frings for sharing data included in the lake and reservoir data sets. We also benefitted from the statistical expertise of UW Statistical Consulting, Igor Markelov, and Jennifer Hood. This work was financially supported by the Canada Excellence Research Chair (CERC) and Ontario Graduate Scholarships (OGS) programs. The GRanD database [*Lehner et al*., 2011] was retrieved online from http://atlas.gwsp.org/index.php?option=com_content&task=view&id=208&Itemid=52. The GLWD database [*Lehner and Döll*, 2004] was retrieved online from http://worldwildlife.org/pages/conservation-science-data-and-tools.

References

Beusen, A. H. W., A. F. Bouwman, H. H. Dürr, A. L. M. Dekkers, and J. Hartmann (2009), Global patterns of dissolved silica export to the coastal zone: Results from a spatially explicit global model, *Global Biogeochem. Cycles*, *23*, GB0A02, doi:10.1029/2008GB003281.

Billen, G., C. Lancelot, and M. Meybeck (1991), N, P, and Si retention along the aquatic continuum from land to ocean, in *Ocean Margin Processes in Global Change*, *Dahlem Workshop Rep*., edited by R. F. C. Mantoura, J. M. Martin, and R. Wollast, pp. 19–44, Wiley, New York.

Brzezinski, M. A., D. R. Phillips, F. P. Chavez, G. E. Friederich, and R. C. Dugdale (1997), Silica production in the Monterey, California upwelling system, *Limnol. Oceanogr.*, *42*(8), 1694–1705.

Carlson, R. E., and J. Simpson (1996), *A Coordinator's Guide to Volunteer Lake Monitoring Methods*, 96 pp., North American Lake Management Society, Madison, Wisc.

Conley, D. J. (1997), Contribution of biogenic silica to the oceanic silica budget, *Limnol. Oceanogr.*, *42*(4), 774–777.

Conley, D. J., C. L. Schelske, and E. F. Stoermer (1993), Modification of the biogeochemical cycle of silica with eutrophication, *Mar. Ecol. Prog. Ser.*, *101*, 179–192.

Conway, H. L., J. I. Parker, E. M. Yaguchi, and D. L. Mellinger (1977), Biological utilization and regeneration of silicon in Lake Michigan, *J. Fish. Res. Board Can.*, *34*(4), 537–544.

Cook, P. L. M., K. T. Aldridge, S. Lamontagne, and J. D. Brookes (2010), Retention of nitrogen, phosphorus and silicon in a large semi-arid riverine lake system, *Biogeochemistry*, *99*, 49–63.

Cornelis, J.-T., B. Delvaux, R. B. Georg, Y. Lucas, J. Ranger, and S. Opfergelt (2011), Tracing the origin of dissolved silicon transferred from various soil-plant systems towards rivers: A review, *Biogeosciences*, *8*, 89–112.

Dai, J., M. Sun, R. A. Culp, and J. E. Noakes (2009), A laboratory study on biochemical degradation and microbial utilization of organic matter comprising a marine diatom, land grass, and salt marsh plant in estuarine ecosystems, *Aquat. Ecol.*, *43*, 825–841.

Davis, C. C., H. Chen, and M. Edwards (2002), Modeling silica sorption to iron hydroxide, *Environ. Sci. Technol.*, *36*(4), 582–587.

Dickson, E. L. (1975), A silica budget for Lough Neagh 1970-1972, *Freshwater Biol.*, *5*, 1–12.

Dürr, H. H., M. Meybeck, J. Hartmann, G. G. Laruelle, and V. Roubeix (2011), Global spatial distribution of natural riverine silica inputs to the coastal zone, *Biogeosciences*, *8*, 597–620.

Friedl, G., C. Teodoru, and B. Wehrli (2004), Is the Iron Gate I reservoir on the Danube River a sink for dissolved silica?, *Biogeochemistry*, *68*, 21–32.

Frings, P. J., W. Clymans, E. Jeppesen, T. L. Lauridsen, E. Struyf, and D. J. Conley (2014), Lack of steady-state in the global biogeochemical Si cycle: Emerging evidence from lake Si sequestration, *Biogeochemistry*, *117*, 255–277, doi:10.1007/s10533-013-9944-z.

Garnier, J., B. Leporcq, N. Sanchez, and X. Philippon (1999), Biogeochemical mass-balances (C, N, P, Si) in three large reservoirs of the Seine Basin (France), *Biogeochemistry*, *47*, 119–146.

Garnier, J., A. Beusen, V. Thieu, G. Billen, and L. Bouwman (2010), N:P:Si nutrient export ratios and ecological consequences in coastal seas evaluated by the ICEP approach, *Global Biogeochem. Cycles*, *24*, GB0A05, doi:10.1029/2009GB003583.

Geddes, M. C. (1984), Limnology of Lake Alexandrina, River Murray, South Australia, and the effects of nutrients and light on the phytoplankton, *Aust. J. Mar. Freshwater Res.*, *35*, 399–415.

Gibson, C. E., G. Wang, and R. H. Foy (2000), Silica and diatom growth in Lough Neagh: The important of internal cycling, *Freshwater Biol.*, *45*, 285–293.

Harrison, J. A., P. J. Frings, A. H. W. Beusen, D. J. Conley, and M. L. McCrackin (2012), Global importance, patterns, and controls of dissolved silica retention in lakes and reservoirs, *Global Biogeochem. Cycles*, *26*, GB2037, doi:10.1029/2011GB004228.

Hartmann, J., and N. Moosdorf (2012), The new global lithological map database GLiM: A representation of rock properties at the Earth surface, *Geochem. Geophys. Geosyst.*, *13*, Q12004, doi:10.1029/2012GC004370.

Hartmann, J., N. Jansen, H. H. Dürr, A. Harashima, K. Okubo, and S. Kempe (2009), Predicting riverine dissolved silica fluxes into coastal zones from a hyperactive region and analysis of their first order controls, *Int. J. Earth Sci.*, *99*(1), 207–230, doi:10.1007/s00531-008-0381-5.

Hartmann, J., J. Levy, and S. Kempe (2011), Increasing dissolved silica trends in the Rhine River: An effect of recovery from high P loads?, *Limnology*, *12*, 63–73.

Hoffman, D. A., P. R. Tramutt, F. C. Heller, and Bureau of Reclamation (1967), Water quality study of Lake Mead. [Available at http://digitalscholarship.unlv.edu/water_pubs/42.]

Horn, H., and W. Horn (2000), Sedimentation—The main loss factor in waters dominated by diatoms, results of long term investigations, *Int. Rev. Hydrobiol.*, *85*, 191–208.

Hughes, H. J., S. Bouillon, L. André, and D. Cardinal (2012), The effect of weathering variability and anthropogenic pressures upon silicon cycling in an intertropical watershed (Tana River, Kenya), *Chem. Geol.*, *308-309*, 18–25.

Humborg, C., D. J. Conley, L. Rahm, F. Wulff, A. Cociasu, and V. Ittekkot (2000), Silicon retention in river basins: Far-reaching effects on biogeochemistry and aquatic food webs in coastal marine environments, *Ambio*, *29*(1), 45–50.

Husnain, T. W., and T. Masunaga (2009), Dissolved silica dynamics and phytoplankton population in Citarum watershed, Indonesia, *J. Food, Agric. Environ.*, *7*(3&4), 132–139.

Iler, R. K. (1979), *The Chemistry of Silica: Solubility, Polymerization, Colloid and Surface Properties, and Biochemistry*, 866 pp., John Wiley, New York.

ISAG (Interim Scientific Advisory Group) (2000), Report on the acid deposition monitoring of EANET during the preparatory phase —Its results, major constraints and ways to overcome them, Acid Deposition Monitoring Network in East Asia. Retrieved online March 6, 2014. [Available at http://www.eanet.asia/product/rep_pre_chapter.pdf.]

Jansen, N., J. Hartmann, R. Laurerwald, H. H. Dürr, S. Kempe, S. Loos, and H. Middelkoop (2010), Dissolved silica mobilization in the conterminous USA, *Chem. Geol.*, *270*, 90–109.

Kelly, V. (2001), Influence of reservoirs on solute transport: A regional-scale approach, *Hydrol. Processes*, *15*, 1227–1249.

Koszelnik, P., and J. A. Tomaszek (2008), Dissolved silica retention and its impacts on eutrophication in a complex of mountain reservoirs, *Water Air Soil Pollut.*, *189*, 189–198.

Krause, J. W., D. M. Nelson, and M. A. Brzezinski (2011), Biogenic silica production and the diatom contribution to primary production and nitrate uptake in the eastern equatorial Pacific Ocean, *Deep Sea Res.*, *58*, 434–448.

Laruelle, G. G., et al. (2009), Anthropogenic perturbation of the silicon cycle at the global scale: Key role of land-ocean transitions, *Global Biogeochem. Cycles*, *23*, GB4031, doi:10.1029/2008GB003267.

Lauerwald, R., J. Hartmann, N. Moosdorf, H. H. Dürr, and S. Kempe (2012), Retention of dissolved silica within the fluvial system of the conterminous USA, *Biogeochemistry*, *112*(1-3), 637–659, doi:10.1007/s10533-012-9754-8.

Le Thi Phuong, Q., G. Billen, J. Garnier, S. Théry, D. Ruelland, X. N. Anh, and C. V. Minh (2010), Nutrient (N, P, Si) transfers in the subtropical Red River system (China and Vietnam): Modelling and budget of nutrient sources and sinks, *J. Asian Earth Sci.*, *37*, 259–274.

Lehner, B., and P. Döll (2004), Development and validation of a global database of lakes, reservoirs and wetlands, *J. Hydrol.*, *296*, 1–22.

Lehner, B., et al. (2011), High resolution mapping of the world's reservoirs and dams for sustainable river flow management, *Front. Ecol. Environ.*, *9*(9), 494–502.

Loucaides, S., P. Van Cappellen, V. Roubeix, B. Moriceau, and O. Ragueneau (2012), Controls on the recycling and preservation of biogenic silica from biomineralization to burial, *Silicon*, *4*, 7–22.

McGinnis, D. F., S. Bocaniov, C. Teodoru, G. Friedl, A. Lorke, and A. Wüest (2006), Silica retention in the Iron Gate I reservoir on the Danube River: The role of side bays at nutrient sinks, *River Res. Appl.*, *22*, 441–456.

Michel, T. J., J. E. Saros, S. J. Interlandi, and A. P. Wolfe (2006), Resource requirements of four freshwater diatom taxa determined by in situ growth bioassays using natural populations from alpine lakes, *Hydrobiologia*, *568*, 235–243.

Mosley, L. M., B. Zammit, E. Leydon, T. M. Heneker, M. R. Hipsey, D. Skinner, and K. T. Aldridge (2012), The impact of extreme low flows on the water quality of the lower Murray River and lakes (South Australia), *Water Resour. Manage.*, *26*, 3923–3946.

Müller, B., M. Berg, B. Pernet-Coudrier, W. Qi, and H. Liu (2012), The geochemistry of the Yangtze River: Seasonality of concentrations and temporal trends of chemical loads, *Global Biogeochem. Cycles*, *26*, GB2028, doi:10.1029/2011GB004273.

Nam, T. N. (1995), The geology of Vietnam: A brief summary and problems, *Geosci. Rep. Shizuoka Univ.*, *22*, 1–10.

Nelson, D. M., P. Tréguer, M. A. Brzezinski, A. Leynaert, and B. Quéguiner (1995), Production and dissolution of biogenic silica in the oceans: Revised global estimates, comparison with regional data and relationship to biogenic sedimentation, *Global Biogeochem. Cycles*, *9*(3), 359–372, doi:10.1029/95GB01070.

Opfergelt, S., E. S. Eiriksdottir, K. W. Burton, A. Einarsson, C. Siebert, S. R. Gislason, and A. N. Halliday (2011), Quantifying the impact of freshwater diatom productivity on silicon isotopes and silicon fluxes: Lake Myvatn, Iceland, *Earth Planet. Sci. Lett.*, *305*, 73–82.

Ran, X., Z. Yu, Q. Yao, H. Chen, and H. Guo (2013), Silica retention in the Three Gorges Reservoir, *Biogeochemistry*, *112*, 209–228.

Redshaw, C. J., C. F. Mason, C. R. Hayes, and R. D. Roberts (1988), Nutrient budget for a hypertrophic reservoir, *Water Res.*, *22*(4), 413–419.

Ryves, D. B., R. W. Battarbee, S. Juggins, S. C. Fritz, and N. J. Anderson (2006), Physical and chemical predictors of diatom dissolution in freshwater and saline lake sediments in North America and West Greenland, *Limnol. Oceanogr.*, *51*(3), 1355–1368.

Saccone, L., D. J. Conley, E. Koning, D. Sauer, M. Sommer, D. Kaczorek, S. W. Blecker, and E. F. Kelly (2007), Assessing the extraction and quantification of amorphous silica in soils of forest and grassland ecosystems, *Eur. J. Soil Sci.*, *58*(6), 1446–1459.

Sauer, D., L. Saccone, D. J. Conley, L. Hermann, and M. Sommer (2006), Review of methodologies for extracting plant-available and amorphous Si from soils and aquatic sediments, *Biogeochemistry*, *80*(1), 89–108.

Schelske, C. L. (1985), Biogeochemical silica mass balances in Lake Michigan and Lake Superior, *Biogeochemistry*, *1*, 197–218.

Schelske, C. L., and E. F. Stoermer (1971), Eutrophication, silica depletion, and predicted changes in algal quality in Lake Michigan, *Science*, *173*, 423–424.

Tavernini, S., E. Pierobon, and P. Viaroli (2011), Physical factors and dissolved reactive silica affect phytoplankton community structure and dynamics in a lowland eutrophic river (Po River, Italy), *Hydrobiologia*, *669*, 213–225.

Teodoru, C., and B. Wehrli (2005), Retention of sediments and nutrients in the Iron Gate I Reservoir of the Danube River, *Biogeochemistry*, *76*, 539–565.

Teodoru, C., A. Dimopoulos, and B. Wehrli (2006), Biogenic silica accumulation in the sediments of Iron Gate I Reservoir on the Danube River, *Aquat. Sci.*, *68*(4), 469–481, doi:10.1007/s00027-006-0822-9.

Thieu, V., G. Billen, and J. Garnier (2009), Nutrient transfer in three contrasting NW European watersheds: The Seine, Somme, and Scheldt Rivers. A comparative application of the Seneque/Riverstrahler model, *Water Res.*, *43*(6), 1740–1754.

Tréguer, P., D. M. Nelson, A. J. Van Bennekom, D. J. DeMaster, A. Leynaert, and B. Quéguiner (1995), The silica balance in the world ocean: A reestimate, *Science*, *268*, 375–279.

Triplett, L. D., D. R. Engstrom, D. J. Conley, and S. M. Schellhaass (2008), Silica fluxes and trapping in two contrasting natural impoundments of the upper Mississippi River, *Biogeochemistry*, *87*, 217–230.

Triplett, L. D., D. R. Engstrom, and D. J. Conley (2012), Changes in amorphous silica sequestration with eutrophication of riverine impoundments, *Biogeochemistry*, *108*, 413–427.

Valiela, I. (1995), *Marine Ecological Processes*, Springer, New York.

Van Cappellen, P. (2003), Biomineralization and global biogeochemical cycles, in *Biomineralization*, *Rev. Mineral. Geochem.*, vol. 54, edited by P. Dove, J. DeYoreo, and S. Weiner, pp. 357–381, Mineral. Soc. Amer., Washington, D. C.

Van Cappellen, P., and L. Qiu (1997), Biogenic silica dissolution in sediments of the Southern Ocean. I. Solubility, *Deep Sea Res., Part II*, *44*(5), 1109–1128.

Van Cappellen, P., S. Dixit, and J. Van Beusekom (2002), Biogenic silica dissolution in the oceans: Reconciling experimental and field-based dissolution rates, *Global Biogeochem. Cycles*, *16*(4), 1075, doi:10.1029/2001GB001431.

Van Donk, E., and S. S. Kilham (1990), Temperature effects on silicon- and phosphorus-limited growth and competitive interactions among three diatoms, *J. Phycol.*, *26*, 40–50.

Wang, F., Y. Yu, C. Liu, B. Wang, Y. Wang, J. Guan, and H. Mei (2010), Dissolved silicate retention and transport in cascade reservoirs in Karst area, Southwest China, *Sci. Total Environ.*, *408*, 1667–1675.

Wetz, M. S., B. Hales, and P. A. Wheeler (2008), Degradation of phytoplankton-derived organic matter: Implications for carbon and nitrogen biogeochemistry in coastal ecosystems, *Estuarine Coastal Shelf Sci.*, *77*, 422–432.

World Climate (2005), Retrieved online Nov. 6, 2013. [Available at www.worldclimate.com.]

Znachor, P., V. Visocká, J. Nedoma, and P. Rychtecký (2013), Spatial heterogeneity of diatom silicification and growth in a eutrophic reservoir, *Freshwater Biol.*, *58*, 1889–1902.